INTERNATIONAL JOURNAL FOR NUMERICAL METHODS IN FLUIDS
Int. J. Numer. Meth. Fluids 2008; **56**:1289–1295
Published online 17 December 2007 in Wiley InterScience (www.interscience.wiley.com). DOI: 10.1002/fld.1692

On restraining convective subgrid-scale production in Burgers' equation

Joop Helder*,† and Roel Verstappen

Institute of Mathematics and Computing Science, University of Groningen, P.O. Box 407, 9700AK Groningen, The Netherlands

SUMMARY

Since most turbulent flows cannot be computed directly from the (incompressible) Navier–Stokes equations, a dynamically less complex mathematical formulation is sought. In the quest for such a formulation, we consider nonlinear approximations of the convective term that preserve the symmetry and conservation properties. The underlying idea is to restrain the convective production of small scales in an unconditionally stable manner, meaning that the approximate solution cannot blow up in the energy norm. In this paper, the method is worked out and tested successfully for Burgers' equation. Copyright © 2007 John Wiley & Sons, Ltd.

Received 5 April 2007; Revised 22 October 2007; Accepted 22 October 2007

KEY WORDS: Burgers' equation; turbulence modeling; vortex stretching; large-eddy simulation; regularization; subgrid-scale restrainment

1. INTRODUCTION

The Navier–Stokes (NS) equations provide an appropriate model for the nonlinear dynamics of turbulence. For an incompressible flow, the equations are

$$\partial_t \mathbf{u} + \mathscr{C}(\mathbf{u}, \mathbf{u}) = -\nabla p + \mathscr{D}(\mathbf{u}) \tag{1}$$

where $\mathbf{u}$ denotes the fluid velocity and p represents the pressure. The dissipative term is given by $\mathscr{D}(\mathbf{u}) = \Delta\mathbf{u}/Re$, where Re denotes the Reynolds number, and the nonlinear, convective term is defined by $\mathscr{C}(\mathbf{u}, \mathbf{v}) = (\mathbf{u}\cdot\nabla)\mathbf{v}$. Attempts at solving turbulent flows directly from the NS equations fail for high Reynolds numbers, because the convective term produces far too many dynamically relevant scales of motion, see, e.g. [1]. In quest of a dynamically less complex mathematical

*Correspondence to: Joop Helder, Institute of Mathematics and Computing Science, University of Groningen, P.O. Box 407, 9700AK Groningen, The Netherlands.
†E-mail: J.A.Helder@math.rug.nl

formulation, approximate models have been devised. In large-eddy simulation (LES), this is done by applying a spatial filter to the NS equations. Today, a large number of LES models exist, see [2] and the references therein.

In this paper, regularization is considered as a mechanism to reduce the complexity of the dynamics [3, 4]. More specifically, we propose to regularize the convective term

$$\partial_t \mathbf{u} + \widetilde{\mathscr{C}}(\mathbf{u}, \mathbf{u}) = -\nabla p + \mathscr{D}(\mathbf{u}) \tag{2}$$

The above regularized system should be more amenable to approximate numerically, while its solution has to approximate the large-scale dynamical behavior of the NS solution. Examples that fall into this concept are the Leray [5] and NS-α model [6]. The regularization method basically alters the nonlinearity to restrain the production of small scales of motion. In doing so, we choose to preserve the symmetry properties that form the basis for the conservation of energy, enstrophy (in 2D) and helicity (in 3D), for details, see [7]. This criterion yields a class of approximations $\widetilde{\mathscr{C}}(\mathbf{u}, \mathbf{v}) = \mathscr{C}_n(\mathbf{u}, \mathbf{v})$, with

$$\mathscr{C}_2(\mathbf{u}, \mathbf{v}) = \overline{\mathscr{C}(\overline{\mathbf{u}}, \overline{\mathbf{v}})} \tag{3}$$

$$\mathscr{C}_4(\mathbf{u}, \mathbf{v}) = \mathscr{C}(\overline{\mathbf{u}}, \overline{\mathbf{v}}) + \overline{\mathscr{C}(\mathbf{u}', \overline{\mathbf{v}})} + \overline{\mathscr{C}(\overline{\mathbf{u}}, \mathbf{v}')} \tag{4}$$

$$\mathscr{C}_6(\mathbf{u}, \mathbf{v}) = \mathscr{C}(\overline{\mathbf{u}}, \overline{\mathbf{v}}) + \mathscr{C}(\mathbf{u}', \overline{\mathbf{v}}) + \mathscr{C}(\overline{\mathbf{u}}, \mathbf{v}') + \overline{\mathscr{C}(\mathbf{u}', \mathbf{v}')} \tag{5}$$

see [8]. Here, the filter operator is denoted by a bar, and a prime is used to indicate the residual. The three approximations $\mathscr{C}_n(\mathbf{u}, \mathbf{v})$ are intrinsically stable, because the energy, enstrophy (in 2D) and helicity are conserved by construction. For a symmetric filter, the difference between the approximations $\mathscr{C}_n$ and $\mathscr{C}$ is of the order ε^n (with $n = 2, 4, 6$), where ε denotes the length of the filter. The Leray model and NS-α model are of the order ε^2.

The evolution of the vorticity $\boldsymbol{\omega} = \nabla \times \mathbf{u}$ resembles that of the NS equations: the only difference is that $\mathscr{C}$ is replaced by the regularization $\mathscr{C}_n$. By analyzing the regularized triad interactions in detail, the filter length can be determined such that the vortex-stretching process stops (approximately) at the grid scale.

In this paper, the regularization method is applied to the 1D Burgers equation. A spectral approach is followed, yet other solution methods may also be used. The analysis is relatively easy for the Burgers equation, while important aspects of the 3D NS equations remain.

2. BURGERS' EQUATION

In the notation of the previous section, the Burgers equation becomes

$$\partial_t u + \mathscr{C}(u, u) = \mathscr{D}(u) \tag{6}$$

where the convective term and the diffusive term are now given by $\mathscr{C}(u, v) = u\partial_x v$ and $\mathscr{D}(u) = \partial_{xx}^2 u / Re$. We consider Equation (6) on an interval Ω with periodic boundary conditions. In Fourier space, the Burgers equation reads

$$\partial_t \hat{u}_k + \mathscr{C}_k(\hat{u}, \hat{u}) = -(k^2/Re)\hat{u}_k + F_k \tag{7}$$

where the forcing term is given by $F_k \equiv 0$ for $k > 1$ and F_1 such that $\partial_t \hat{u}_1 = 0$ for all t. Here, $\hat{u}_k(t)$ denotes the kth Fourier coefficient of $u(x, t)$ and the nonlinear term consists of all interactions

DOI: 10.1002/fld

between modes $\hat{u}_p$ and $\hat{u}_q$ with $p+q=k$, i.e. $\mathscr{C}_k(\hat{u},\hat{u})=\sum_{p+q=k}\hat{u}_p \mathrm{i}q\hat{u}_q$. The energy e_k of mode k is obtained by taking the product of $\hat{u}_k$ with its complex conjugate $\hat{u}_k^*$.

3. SUBGRID-SCALE PRODUCTION

In a numerical simulation, the production of smaller scales should stop at the smallest scale that can be represented correctly on the computational grid. On a uniform grid with spacing h, the smallest scale is characterized by the cut-off wavenumber $k_c=\pi/h$. By considering the evolution of $\partial_x u$, the process responsible for the small-scale production is further analyzed. The kth Fourier mode of $\partial_x u$ has coefficient $\mathrm{i}k\hat{u}_k$. If this coefficient is magnified (i.e. $k^2\hat{u}_k\hat{u}_k^*$ increases), a smaller scale is produced since the increase in slope leads to a steepened up velocity profile. If the mode under consideration has wavenumber k_c, a magnification of $\mathrm{i}k_c\hat{u}_{k_c}$ produces a mode that cannot be represented correctly on the computational grid, since it has a wavenumber larger than k_c. Hence a magnification of $\mathrm{i}k_c\hat{u}_{k_c}$ introduces numerical error (see Figure 1).

The above-described process in 1D can be compared with the so-called *vortex-stretching mechanism* in 3D, where a magnification of the vorticity vector $\boldsymbol{\omega}$ is responsible for the production of smaller scales. Motivated by this analogy, we further consider the evolution of $\omega\equiv\partial_x u$. Its Fourier modes have coefficients $\hat{\omega}_k=\mathrm{i}k\hat{u}_k$, and the evolution of its magnitude $\hat{\omega}_k\hat{\omega}_k^*$ at the smallest grid scale is given by

$$\partial_t(\hat{\omega}_{k_c}\hat{\omega}_{k_c}^*)=-(2k_c^2/Re)\hat{\omega}_{k_c}\hat{\omega}_{k_c}^*-\mathrm{i}k_c(\hat{\omega}_{k_c}^*\mathscr{C}_{k_c}(\hat{u},\hat{u})-\hat{\omega}_{k_c}\mathscr{C}_{k_c}(\hat{u},\hat{u})^*) \tag{8}$$

where again k_c denotes the cut-off wavenumber of the numerical solution, and a superscript $*$ denotes the complex conjugate. No magnification of $\mathrm{i}k_c\hat{u}_{k_c}$ requires that $\partial_t(\hat{\omega}_{k_c}\hat{\omega}_{k_c}^*)\leqslant 0$. Since the diffusive contribution $-(2k_c^2/Re)\hat{\omega}_{k_c}\hat{\omega}_{k_c}^*$ is negative, this condition reads

$$c\leqslant 0 \quad \text{or} \quad c\geqslant 1 \quad \text{with} \quad c\stackrel{\text{def}}{=}\frac{2\mathrm{i}k_c\hat{\omega}_{k_c}\hat{\omega}_{k_c}^*}{(\hat{\omega}_{k_c}^*\mathscr{C}_{k_c}(\hat{u},\hat{u})-\hat{\omega}_{k_c}\mathscr{C}_{k_c}(\hat{u},\hat{u})^*)Re} \tag{9}$$

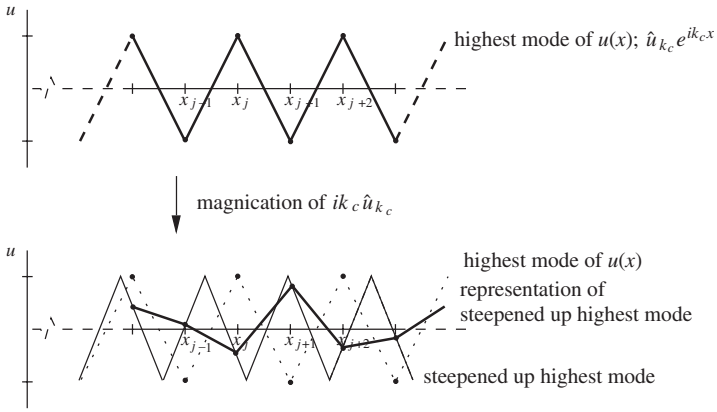

Figure 1. The highest mode of the velocity that can be represented correctly on the computational grid (above) produces a steepened up profile (below), and introduces a numerical error.

DOI: 10.1002/fld

Note that this condition is necessary to stop the highest-frequency mode from producing subgrid scales. To what extend the possible energy flow from lower-frequency modes to subgrid scales (due to strongly nonlinear interactions) is restrained, will become clear from the results.

4. RESTRAINING METHOD

If Condition (9) holds, no scales of motion smaller than the meshsize are produced by the convective term, and Equation (7) can be solved directly. However, if (9) does not hold, the convective production of subgrid scales has to be restrained. To that end, we consider the approximation given by Equation (4). In Fourier space, the convective term is then approximated by

$$\mathscr{C}_{4,k}(\hat{u},\hat{v}) = \sum_{p+q=k} f(\widehat{G}_k,\widehat{G}_p,\widehat{G}_q) \quad \hat{u}_p \mathrm{i} q \hat{v}_q \tag{10}$$

where $\widehat{G}_k$ denotes the Fourier transform of the kernel of the convolution filter and

$$f(\widehat{G}_k,\widehat{G}_p,\widehat{G}_q) = \widehat{G}_k(\widehat{G}_p+\widehat{G}_q)+\widehat{G}_p\widehat{G}_q(1-2\widehat{G}_k) \tag{11}$$

This function satisfies $f(1,1,1)=1$ and $f(0,0,0)=0$. Furthermore, all the first-order partial derivatives of $f(\widehat{G}_k,\widehat{G}_p,\widehat{G}_q)$ are strictly positive for $0<\widehat{G}_k,\widehat{G}_p,\widehat{G}_q<1$. Hence, the factor $f(\widehat{G}_k,\widehat{G}_p,\widehat{G}_q)$ by which every nonlinear interaction is reduced is a monotone function of $\widehat{G}_k$, $\widehat{G}_p$, and $\widehat{G}_q$. In general, the value of the reduction factor $f(\widehat{G}_k,\widehat{G}_p,\widehat{G}_q)$ depends on p and q; hence, the terms in the summation in the right-hand side of (10) are damped differently. To avoid this, a discrete 5-point filter in physical space is constructed such that for $k=k_\mathrm{c}$ the function $f(\widehat{G}_{k_\mathrm{c}},\widehat{G}_p,\widehat{G}_q)$ is almost independent of p and q. Then, $\mathscr{C}_{4,k_\mathrm{c}}(\hat{u},\hat{u}) \approx \tilde{f}(\widehat{G}_{k_\mathrm{c}})\mathscr{C}_{k_\mathrm{c}}(\hat{u},\hat{u})$, and the value of the function $\tilde{f}$ follows from Condition (9) with $\mathscr{C}_{k_\mathrm{c}}$ replaced by $\mathscr{C}_{4,k_\mathrm{c}}$:

$$\tilde{f}(\widehat{G}_{k_\mathrm{c}}) = \frac{2\mathrm{i}k_\mathrm{c}\hat{\omega}_{k_\mathrm{c}}\hat{\omega}^*_{k_\mathrm{c}}}{(\hat{\omega}^*_{k_\mathrm{c}}\mathscr{C}_{k_\mathrm{c}}(\hat{u},\hat{u})-\hat{\omega}_{k_\mathrm{c}}\mathscr{C}_{k_\mathrm{c}}(\hat{u},\hat{u})^*)Re} \tag{12}$$

Note that (i) the right-hand side of (12) equals c, and (ii) the same condition can also be derived from the energy equation, since $\hat{\omega}_k\hat{\omega}^*_k = k^2\hat{u}_k\hat{u}^*_k$. With the help of this relation, the equation for $\hat{\omega}_k\hat{\omega}^*_k$ can be easily transferred into the energy equation, and *vice versa*. We continue by considering the energy: if the Burgers equation is integrated in time with the help of the forward Euler scheme, the discrete time evolution of the energy is given by

$$\frac{[\hat{u}_k]^{n+1}[\hat{u}^*_k]^{n+1}-[\hat{u}_k]^n[\hat{u}^*_k]^n}{\delta t} = [\hat{u}^*_k]^n[W_k]^n+[\hat{u}]^n_k[W^*_k]^n+\delta t[W_k]^n[W^*_k]^n \tag{13}$$

where n and $n+1$ denote the old and new time levels, respectively, $W_k = -\mathscr{C}_{4,k}(\hat{u},\hat{u})-(k^2/Re)\hat{u}_k$, and δt denotes the time step. The last term in the right-hand side of (13) is not taken into account if (12) is simply evaluated at time level n. Therefore, we propose to modify (12) such that the condition holds exact for the time-integration method under consideration.

DOI: 10.1002/fld

5. RESULTS

The approximation $\mathscr{C}_4$ is used to solve the Burgers equation with $Re=50$. As initial condition, $\hat{u}_k = k^{-1}$ has been taken. Since mode $k=0$ has no interaction with other modes, we assume that $\hat{u}_0 = 0$, i.e. there is no mean flow. Figure 2 shows the energy spectrum of the steady state for $k_c = 20$, with and without the regularization method. A time step of $\delta t = 0.001$ has been used, and for the approximation method Equation (12) has been modified using the time-discrete evolution given by (13). A DNS spectrum with $k_c = 100$ and $\delta t = 0.0005$ has been added as a reference. Clearly, for $k_c = 20$ the direct simulation without the model is not able to capture the physics correctly, as the energy is not dissipated enough at the high wavenumbers, and is reflected back towards the larger scales. The inset in Figure 2 illustrates that the direct simulation with $k_c = 20$ is already a substantial amount off the reference DNS for $k=4$. The regularization model shows a characteristic feature; due to energy conservation, the model compensates the energy loss at the smaller scales by an additional hump in the spectrum, just before the fall-off commences.

To investigate the influence of the last term in the right-hand side of (13), a simulation is done with and without this term, again for $k_c = 20$. Figure 3 shows the steady-state energy spectrum as well as the time evolution of the highest mode $\hat{u}_{k_c}$, for both simulations. Using (12) without taking the time-integration method into account, the energy at the highest mode is still able to grow; hence, producing smaller scales of motion. With modification, i.e. when $\tilde{f}$ is evaluated according to (13), the energy is monotonically decreasing, and no modes smaller than $\hat{u}_{k_c}$ are produced. Furthermore, Figure 3 illustrates that for most of the simulation time, the regularization model is turned on, corresponding with the horizontal sections in Figure 3. Only for short periods of time the model is turned off, and energy is dissipated at the highest wavenumber.

Also, the energy spectra for a range of values for k_c have been computed using the regularization method with time-discrete modification. Results for $k_c = 20, 30, 40, 50$ are shown in Figure 4, again

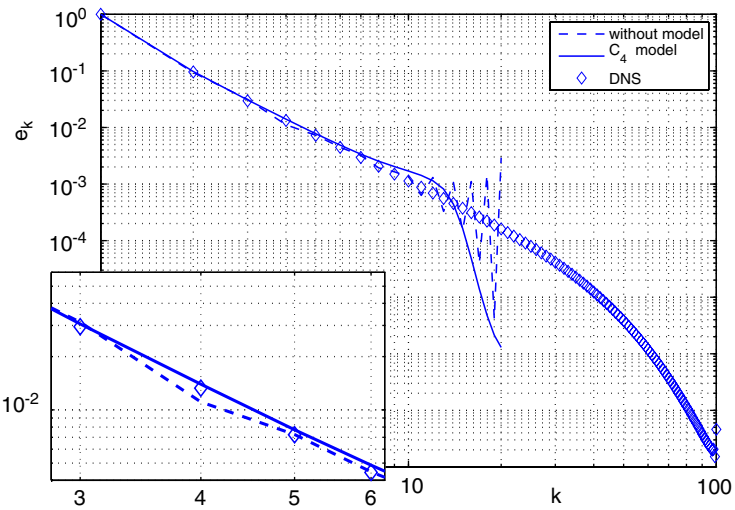

Figure 2. Energy spectrum of the steady-state solution of the Burgers equation, with and without the model, for $k_c = 20$ and $\delta t = 0.001$. The steady state was reached at $t=3$, approximately.

DOI: 10.1002/fld

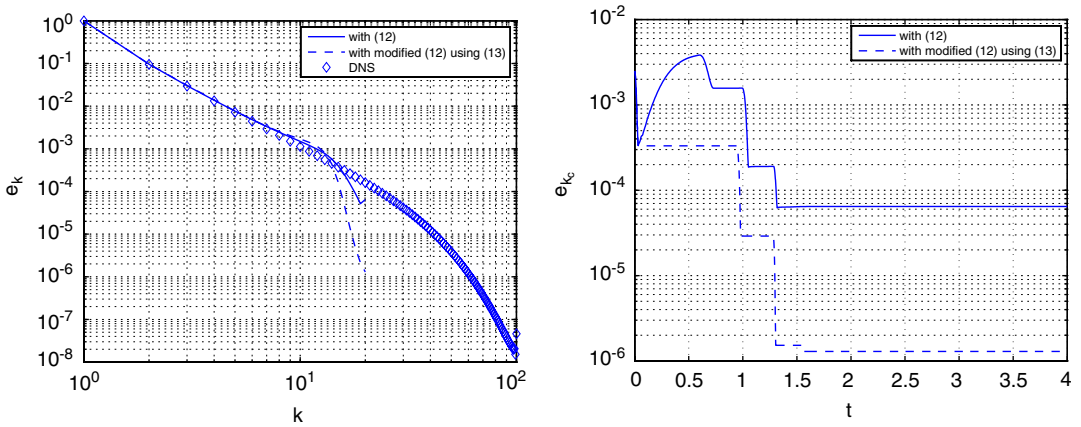

Figure 3. Results using both the model with and the model without the last term in the right-hand side of (13). Left: as in Figure 2. Right: evolution of the energy at the highest wavenumber e_{k_c}.

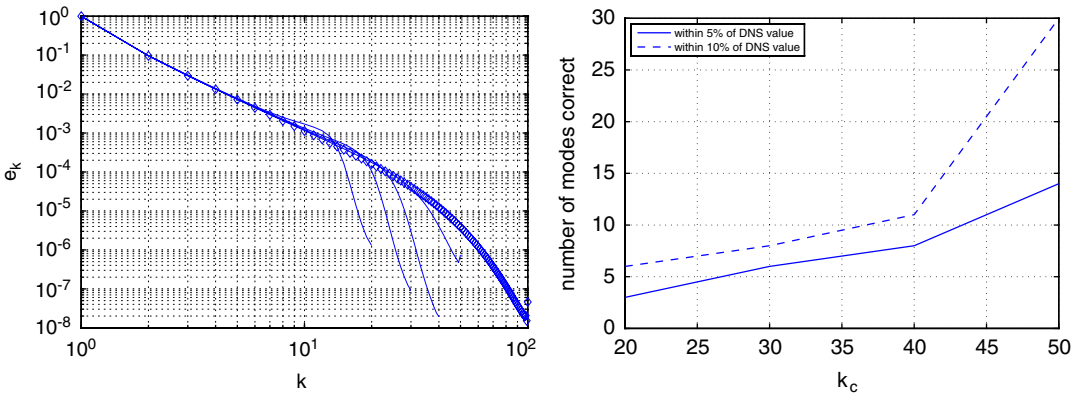

Figure 4. Left: as Figure 2, but now for $k_c = 20, 30, 40, 50$. Right: number of modes represented correctly by the model as a function of k_c. Both an error tolerance of 5 and 10% of the DNS are shown.

using a time step of $\delta t = 0.001$. For smaller values of k_c, the spectra at the high wavenumbers show an almost identical fall-off behavior, proportional to k^{-20}, approximately. This rapid fall-off is a desirable feature of the method, since it yields a small fall-off range of wavenumbers and hence the approximate solution is more likely to collapse with the DNS for a wider wavenumber range. For larger values of k_c, the tail of the spectrum shows a more moderate behavior, converging to the k^{-10} tail of the spectrum of the DNS. Also, Figure 4 shows the number of modes that are still represented correctly by the model as a function of k_c. Both an error tolerance of 5 and 10% are shown. Note that the jump in the 10% tolerance at $k_c \approx 40$ is due to the fact that for larger values of k_c, the complete range of wavenumbers with an overshoot in the spectrum is within 10% of the DNS. For the 5% tolerance, a similar jump has been observed at $k_c > 50$.

DOI: 10.1002/fld

REFERENCES

1. Spalart PR. Strategies for turbulence modeling and simulations. *International Journal of Heat and Fluid Flow* 2000; **21**:252–263.
2. Sagaut P. *Large Eddy Simulation for Incompressible Flows*. Springer: Berlin, 2001.
3. Guermond JL, Oden JT, Prudhomme S. Mathematical perspectives on large eddy simulation models for turbulent flow. *Journal of Mathematical Fluid Mechanics* 2004; **6**:194–248.
4. Geurts BJ, Holm DD. Regularization modeling for large-eddy simulation. *Physics of Fluids* 2003; **15**:L13–L16.
5. Leray J. Sur les movements d'un fluide visqueux remplaissant l'espace. *Acta Mathematica* 1934; **63**:193–248.
6. Holm DD, Marsden JE, Ratiu TS. The Euler–Poincaré equations and semidirect products with applications to continuum theories. *Advances in Mathematics* 1998; **37**:1–81.
7. Foias C, Manley O, Rosa R, Temam R. *Navier–Stokes Equations and Turbulence*. Cambridge University Press: Cambridge, 2001.
8. Verstappen R. On restraining the production of small scales of motion in a turbulent channel flow. *Computers and Fluids*. DOI: 10.1016/j.compfluid.2007.01.013 (Available online 1 October 2007).

DOI: 10.1002/fld